ESR Relaxation Studies on Orbitally Degenerate Free Radicals. II*

M. R. Das, Stephen B. Wagner, and J. H. Freed
Department of Chemistry, Cornell University, Ithaca, New York 14850
(Received 13 October 1969)

Careful linewidth and saturation studies were performed on several orbitally degenerate hydrocarbon free radicals in liquid solution as a function of temperature, solvent, and counterion, and these are compared with similar studies on nondegenerate hydrocarbon free radicals. The anomalous T_1's and T_2's attributed to the orbital degeneracy are found to be strikingly independent of all these variables. This is most clearly evidenced for the coronene and triphenylene anion radicals. The results for the benzene and cyclooctatetraene anions (alkali metal prepared) are complicated by a further contribution to T_2^{-1} which increases with temperature. This contribution is correlated with counterion and solvent dependent ion-pairing effects. The intrinsic temperature-independent T_2^{-1}'s for the orbitally degenerate free radicals are surprisingly well correlated with the small but anomalous deviations of the g values for these radicals from the Segal, Kaplan, and Fraenkel experimental fit to Stone's theory of g values. This is taken as positive evidence for the role of anomalous spin–orbit interactions in the mechanism(s) yielding the anomalous relaxation times. Their independence of temperature, solvent, and counterion suggests that the relaxation mechanism(s) is largely intramolecular.

I. INTRODUCTION

In Part I of this series[1] a study of the T_1 and T_2 properties of two radicals with degenerate ground states, the benzene anion and the tropenyl radical, were presented. The main conclusions of that work were that $T_1 \cong T_2$ for the benzene anion over a wide range of temperatures, and for the tropenyl radical, T_1 also equals T_2. A second observation was the unusual temperature independence of the tropenyl radical linewidth over a wide range of temperatures as well as for the benzene anion below about -85°C. From an analysis of these results of Part I, in terms of our current understanding of a variety of spin-relaxation mechanisms, it was possible to rule out many of the more common mechanisms such as g-tensor and anisotropic dipolar effects, hyperfine fluctuations, and even spin–rotational effects of a conventional sort from consideration in explaining the anomalously strong relaxation of these degenerate ground state free radicals.

The two observations of T_1 tending to equal T_2, and both tending to be rather temperature independent, were not unequivocal from that study, so a continuation of that work was carried out, in part to investigate to what extent these observations are appropriate for other free radicals with degenerate ground states. For these purposes, we have carefully studied the relaxation properties of triphenylene, coronene, and cyclooctatetraene anion radicals. While it is well known that nondegenerate ground-state hydrocarbon free radicals like the naphthalene and anthracene anions have much narrower widths, we thought it would also be interesting to study their typical T_1 behavior for comparison with the other work. It was pointed out in Part I that the perinaphthenyl radical, while it has a nondegenerate ground state, serves as a useful example of a symmetric top free radical, a characteristic shared by all the degenerate free radicals by virtue of their high symmetry, so it was also included in this study.

There have been a number of proposals of relaxation mechanisms to attempt to explain the anomalous widths of the ground-state degenerate free radicals and which invoke considerations of solvent (and counterion) interaction with the free radical.[2–5] The benzene radical studied in Part I was not readily amenable to preparation under a variety of conditions of solvent and counterion, but a preliminary result of Lawler *et al.*[6] has indicated that at least for the linewidths, there seems to be little difference at a given temperature between the low-viscosity dimethoxyethane solvent and the higher-viscosity tetraglyme solvent. We have extended the benzene anion work by performing relaxation measurements of this radical in tetraglyme and solvents like 4-methyl-THF and mixtures of methyl-THF and DME. We have also made use of the new ENDOR and ELDOR techniques in studying the relaxation characteristics of the benzene anion.

The radicals triphenylene, coronene, and cyclooctatetraene can be made in a variety of solvents with different counterions. So, it was possible for us to study the effects of these variables. Similar studies were also made in the cases of naphthalene, tetracene, and the neutral perinaphthenyl.

One can also, in trying to understand the relaxation mechanisms for the degenerate ground-state free radicals, ask the question about the role that a small static perturbation, which lifts the degeneracy, can play on the relaxation mechanisms. One notes from the careful studies on deuterated benzenes, including monodeuterobenzene, that such a static perturbation has no significant effect in reducing the magnitude of the benzene linewidths.[7] On the other hand, one notes that for free radicals like the toluene and p-xylene anions wherein methyl groups supply larger static perturbations, there is a significant decrease in the observed linewidths. Studies of T_1 on these latter two free radicals are somewhat complicated by significant overlap in the spectrum. However, we were able to

make some progress in the case of *p*-xylene and have included it for purposes of comparison with the other radicals.

We might also note that in the cases of triphenylene and coronene, there also was a significant overlap problem. This is a problem which has only a small effect on the observed splitting constants, changing them by about 3% from the true splitting constant values. However, as will be seen in this work, such small overlap effects nevertheless have major effects in terms of the true versus observed linewidth, and more important, the rate of change of the overlapped linewidth with increase in microwave power which causes saturation broadening. We have made use of computer simulation techniques to overcome the basic difficulties posed by this problem.

Our experimental techniques are briefly described in Sec. II. The experimental results are given in Sec. III and discussed in Sec. IV.

II. MATERIALS AND METHODS

Benzene used in the present experiments was Fisher spectranalyzed material and was used without further purification. Naphthalene and *p*-xylene were Eastman White Label quality. Naphthalene was sublimed twice, and *p*-xylene was dried over Na–K alloy before use. Coronene, triphenylene, and tetracene were from Aldrich Chemical Company and were used without further purification. Cyclo-octatetraene (COT) was from K&K Laboratories and was purified by vacuum distillation before use. Perinaphthenyl was prepared from perinaphthenone (Aldrich) by lithium aluminum hydride reduction according to the method of Boekelheide and Larrabee.[8] 1,2-Dimethoxyethane (DME), tetrahydrofuran (THF), 4-methyl-tetrahydrofuran (MTHF), and bis-[2-(2-methoxy-ethoxy)ethyl]ether (tetraglyme, TG) were obtained from Eastman Organic Chemicals and were purified according to methods described previously.[6,9,10] Tetra-*n*-butylammonium perchlorate (TBAP) was obtained from Southwestern Analytical Chemicals, and the material was purified by drying the wet product in a vacuum desiccator over P_2O_5, and then recrystallizing it from anhydrous ethylacetate.

The anion radicals from benzene and *p*-xylene were produced by reduction with Na–K alloy in different solvents using well-known techniques.[10,11] Radicals from naphthalene, tetracene, coronene, triphenylene, and cyclo-octatetraene were generated by standard techniques[10,12–14] using a mirror of the alkali metal in the case of Na and K. For lithium reduction a weighed piece of the metal was employed without making a mirror. Electrolytic reduction of COT was carried out in a cell similar to the one described by Bolton and Fraenkel.[10] However, in the present case a platinum cathode was employed. The solution of COT in DME containing 0.1*M* TBAP was electrolyzed at a potential of −2.2 V with respect to the silver–silver percholate reference electrode.[6]

The sample of perinaphthenyl in toluene was made by dissolving the required amount of perinaphthenyl in toluene which had been dried over sodium wire and then degassing the sample thoroughly. The DME sample was made by distilling purified DME into the sample tube containing the necessary amount of perinaphthenyl under vacuum.

The X-band ESR spectrometer employed in the present experiments, and the experimental procedure for measuring relaxation times using continuous saturation have already been described.[1,15] All the present measurements have been made using a modulation frequency of 6 kHz,[15] and the magnetic field was stabilized with a Varian field-frequency lock. The method of determining the Q values of the cavity has also been described in Part I.

The g value of triphenylene was determined relative to the values reported by Kaplan, Segal, and Fraenkel,[16] using two independent standards, viz., naphthalene–Na in DME and p-benzosemiquinone anion at room temperature.

The ENDOR and ELDOR techniques are described elsewhere.[17,18]

III. EXPERIMENTAL RESULTS

The method of determining the relaxation times using progressive saturation techniques is based on the expression[19]

$$\delta^2=(4/3\gamma^2)\,(1/T_2)^2+\tfrac{4}{3}B_1^2(T_1/T_2), \qquad (3.1)$$

where δ is the derivative peak-to-peak width, γ is the gyromagnetic ratio of the electron, and B_1 is the circularly polarized magnetic induction at the sample which is given by[19,20]

$$B_1^2=(\mu Q_0/4\pi\nu_0)H_0^2P_{\rm inc}(1-|\Gamma_0|^2)\,(Wb^2/MA). \qquad (3.2)$$

In Eq. (3.2) Q_0 is the unloaded cavity Q, ν_0 is the cavity resonance frequency, and $P_{\rm inc}$ is the microwave power incident on the cavity. Γ_0 is the power reflection coefficient for the cavity at resonance, and H_0^2 is the reduced magnetic field strength. The experimental fits to Eq. (3.1) yielded values for T_2 with a precision of 1%–4% and T_1/T_2 with 8%–20% precision in the present work. In all cases, only the central line or lines was studied.

A. Q Values

In order to determine the relaxation times, the values for the quantity $Q_0(1-|\Gamma_0|^2)$ in Eq. (3.2) were determined for the different solvent systems as a function of temperature. The values for a 3-mm-o.d. sample tube are reported in Table I. It may be noted that in most of the cases reported in Table I it was possible to obtain perfect match, i.e., $|\Gamma_0|^2=0$. For DME and THF solutions, there was very slight mismatch below

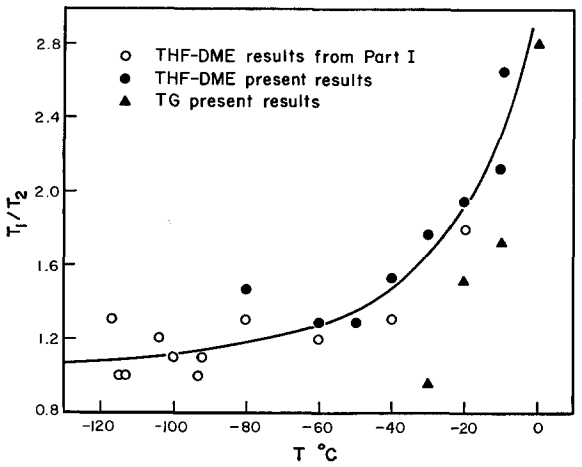

FIG. 1. Variation of T_1/T_2 ratio for benzene anion as a function of temperature.

-70°C, and in these cases $|\Gamma_0|^2$ is finite, but nevertheless small.

B. Width and Saturation Results[21]

1. *Hydrocarbon Anions with Degenerate Ground States*

a. Benzene. We have made several measurements of relaxation times of benzene in a mixture of THF–DME at relatively higher temperatures than those reported in Part I, and our results together with the earlier results are shown in Figs. 1 and 2. These figures also

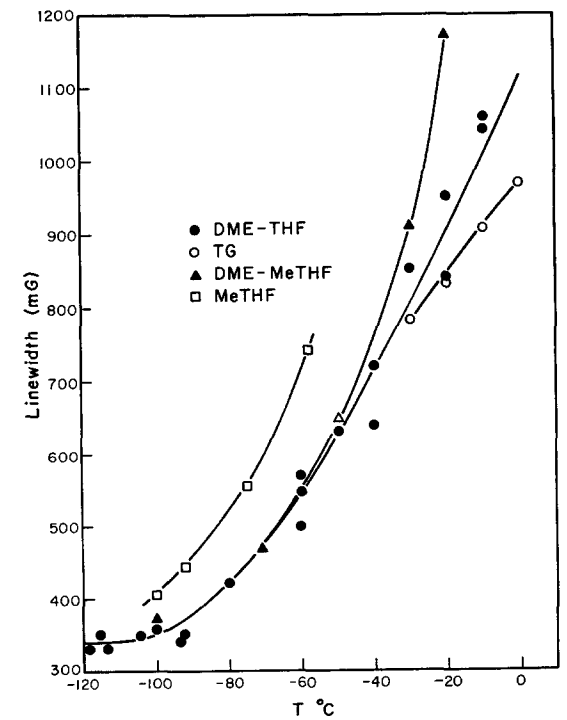

FIG. 2. Linewidth variations for benzene anion in different solvents as a function of temperature (0.3 M in benzene).

TABLE I. $Q_0(1-|\Gamma_0|^2)$.

Solvent system	$Q_0(1-\|\Gamma_0\|^2)$[a,b]	Temp. range (°C)
Toluene	$(6187\pm464.)-(16\pm10.)t$[c]	(-80)–$(+23)$
Tetraglyme	$(3935\pm63.)-(24\pm3.)t$	(-30)–$(+23)$
Dimethoxyethane (DME)	$(3857\pm63.)+(20\pm2.)t$	(-70)–$(+23)$
Tetrahydrofuran (THF)	$(4603\pm151.)+(17\pm4.)t$	(-100)–$(+23)$
2:1 THF:DME	$(4693\pm60.)+(26\pm1.)t$	(-80)–$(+23)$

[a] Γ_0 was minimized for each solvent/temperature system (see text).
[b] Errors are sample deviations.
[c] Temperatures are in degrees centigrade.

contain our results on measurements using tetraglyme (TG) as solvent. As TG freezes below -30°C, low-temperature measurements in solution are not possible using this solvent. Figure 1 is a plot of T_1/T_2 as a function of temperature for benzene anion in a mixture of THF–DME and also in TG. The small differences in the results with the two solvents above -25°C are probably not experimentally very significant in view of the scatter. Figure 2 is a plot of the variation of linewidth (peak-to-peak derivative width of the central component of benzene anion spectrum) as a function of temperature. Results on four different solvent systems are included in this plot: THF–DME (2:1),

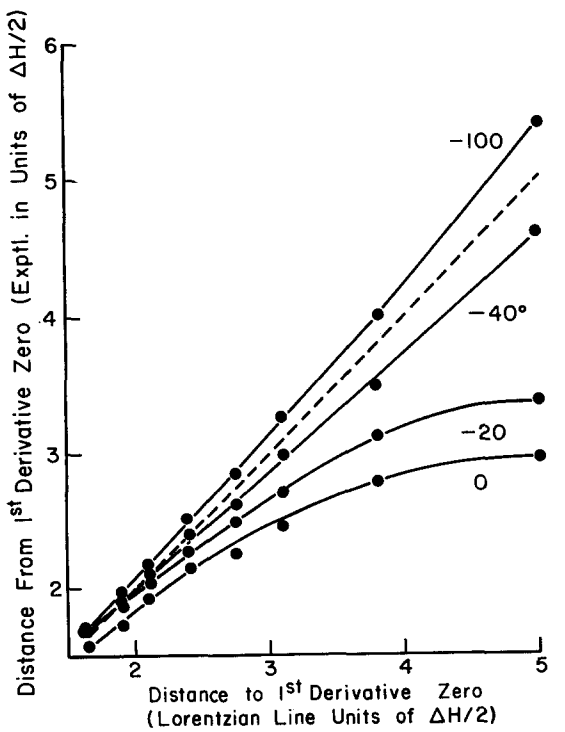

FIG. 3. Line shapes of the $M_H=0$ component in the first derivative ESR spectrum of benzene anion in THF–DME mixture at different temperatures (0.3 M in benzene). Dotted line corresponds to a theoretical Lorentzian line (cf. Ref. 15).

TG, MTHF–DME (4:1), and pure MTHF. Here, there are small but significant solvent dependent effects on the widths. We have also studied the benzene line shape as a function of temperature, at the higher temperatures. The line-shape shifts from decaying more slowly in the wings at −100°C to decaying more rapidly at the higher temperatures, as compared to a Lorentzian (cf. Fig. 3). It may be noticed that even at the higher temperatures there were no significant corrections that were found to be necessary for overlap of the hyperfine components in the benzene spectrum. Our ability to perform careful line shape studies, especially at higher temperatures, was due in part to the enhanced field stability provided by the field-frequency lock.

b. Coronene. The ESR spectrum for the coronene negative ion has been reported by earlier workers.[22] We have obtained the coronene anion in DME and THF using different alkali metals, viz., Na and K. The width of a hyperfine line for a dilute solution of coronene anion was found to be independent of the counterion or the solvents.

Although a width of 700 mg for coronene negative ion has been reported earlier,[22] the measured derivative width in the present case for dilute solutions were slightly lower (≈650 mg). However, when we tried to simulate the ESR spectrum using the measured width and splitting constants and assuming a Lorentzian line shape, the shape of the experimental spectrum was not reproduced satisfactorily. There is considerable overlap in the experimental spectrum, and hence when larger widths were employed for the computer simulation, good agreement was obtained. For example, for the coronene anion spectrum (Li–THF, −20°C) using a width of 0.860 G and a splitting $a^H=1.484$ G we were able to obtain a perfect fit with the experimental spectrum assuming a Lorentzian shape for the lines. Clearly, the experimentally observed linewidths

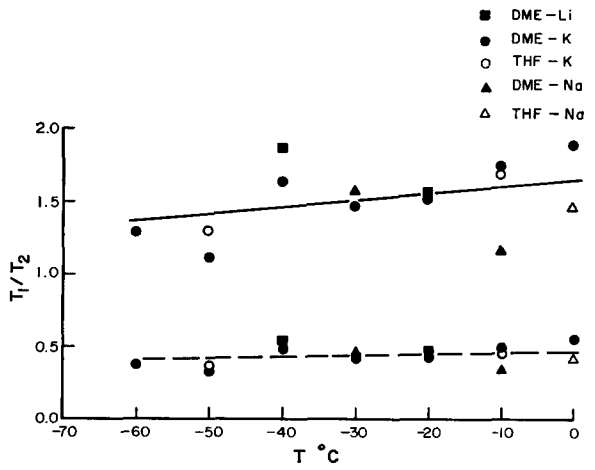

FIG. 4. T_1/T_2 ratio for coronene anion as a function of temperature, solvent, and counterion.

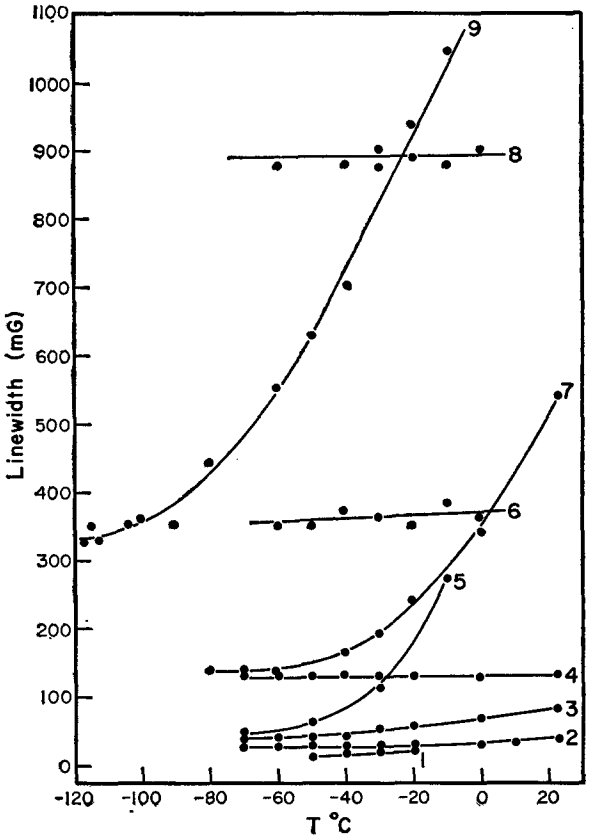

FIG. 5. Linewidth variations in the ESR spectra of several hydrocarbon negative ions and K^+TCNE^- as a function of temperature. (1) Perinaphthenyl in toluene (10^{-4} *M* at 23°C, see text); (2) K^+TCNE in DME, 10^{-4} *M*; (3) tetracene–Li in DME, 10^{-4} M; (4) COT–electrolytic in DME (dilute solution, see text); (5) naphthalene–Na in DME, 10^{-4} *M*; (6) triphenylene anion, $\approx 10^{-4}$ *M* (widths independent of solvent and counterion, see text); (7) COT–Li in THF (concentrated sample, see Curve No. 7 in Figs. 9 and 10); (8) coronene anion, $\approx 10^{-4}$ *M* (widths independent of solvent and counterion, see text); (9) benzene anio in THF–DME (2:1 mixture).

cannot be employed for calculating T_1 and T_2. In order to circumvent this difficulty, the following procedure was adopted. Computer simulations of the spectrum were made in which the experimental splitting constant was utilized, but a different linewidth was employed for each simulation (i.e., 0.75–1.30 G at 20-mG intervals). For each input (true width) a peak-to-peak derivative width from the computed spectrum corresponding to the experimentally measured width was obtained. A plot was made with the true (input) width versus the peak-to-peak width, and it was found to be linear in the region of interest. The result yielded a least-squares fit for a straight line according to

$$\delta_{\text{true}}=(2.639\pm0.024)\,\delta_{\text{measured}}-(0.961\pm0.018)\ \text{G}. \tag{3.3}$$

In order to obtain the corrected T_1 and T_2, the experimentally measured peak-to-peak widths were corrected using Eq. (3.3). Figure 4 shows the results on the

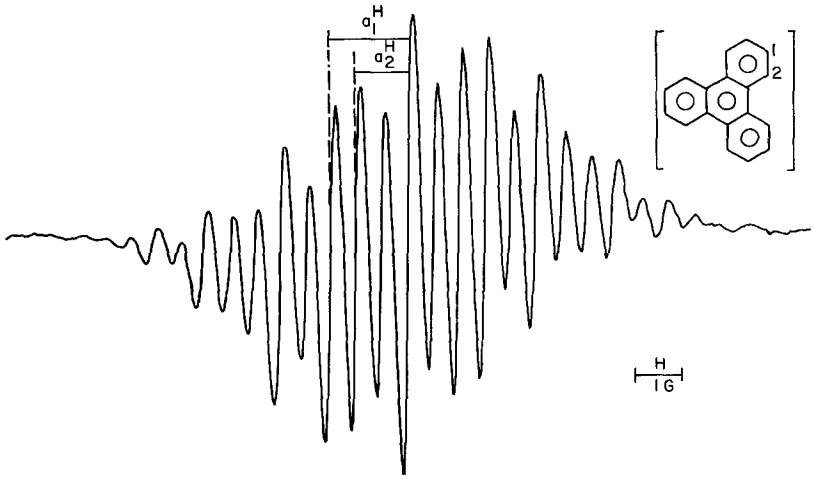

FIG. 6. First derivative ESR spectrum of triphenylene–Li in DME at −80°C.

variation of T_1/T_2 versus temperature, counterion, and solvent for coronene. The upper curve gives the corrected T_1/T_2, and the points in the lower curve are obtained from the uncorrected peak-to-peak widths. It may be noticed that in either case the T_1/T_2 values do not show any significant variation with temperature, counterion, or solvent. The significantly larger absolute scatter of the adjusted data in the upper curve may be attributed mainly to the factor of nearly 4 increase in value of T_1/T_2. Relative scatter about the mean is nearly the same in both cases. There is, however, some further percent error introduced into the individual δ_{true} values used in each T_1/T_2 analysis as a result of applying Eq. (3.3). The results for the true relaxation times (upper curve) may be fitted as a function of temperature according to

$$T_1/T_2=(1.62\pm0.09)+0.0043\pm0.0030)t\ ^\circ\text{C}. \quad (3.4a)$$

The temperature-dependent term in Eq. (3.4a) is hardly significant. Figure 5, which contains typical linewidth variations in the ESR spectra of the hydrocarbon anions we have investigated, also shows the true widths for coronene negative ion as a function of temperature. A linear least-squares fit of T_2 versus temperature gave

$$T_2=[(0.074\pm0.01)-(0.0002\pm-0.0002)t\ ^\circ\text{C}]\times10^{-7}, \quad (3.4b)$$

or a temperature-independent result as well.

c. Triphenylene. The ESR spectrum from triphenylene (TP) anion has been reported by Townsend and Weissman.[22] However, their spectrum was not well resolved, and correct splitting constants could not be obtained from it.[22a] We were able to obtain improved resolution of the spectrum in DME and THF using Li, Na, and K for reduction. As in the case of coronene, the minimum width obtained for TP showed no variation with the counterions or solvents mentioned above. Also the widths remained invariant as a function of temperature.

The ESR spectrum of TP (Li–THF at −80°) is shown in Fig. 6. The spectrum can be interpreted in terms of two splitting constants from positions 1 and 2 (see Fig. 6). The splitting constants are $a_1^H=1.635$ G and $a_2^H=1.080$ G at −80°C, and $a_1^H=1.616$ G and $a_2^H=1.079$ G at −20°C for a dilute solution of TP in THF with Li as the counterion. The splitting constants are essentially unchanged when Na or K is used for reduction. Any variation in the splittings is negligible when DME is used in place of THF. The g value of the sample was determined to be 2.002823 ± 0.000008. As in the case of the hyperfine splittings, there was no change in the g values with different counterions in DME and THF within experimental error. It is interesting to note that although one does expect two splittings from TP from symmetry considerations, a simple HMO calculation or a calculation including the McLachlan correction[23] yielded the same spin density[24] at all the proton positions in the molecule (0.056). On the other hand, a calculation using the Pariser–Parr–Pople-type SCF calculation[25] yielded two different values,[26] $\rho_1=0.061$ and $\rho_2=0.042$. The ratio of these calcu-

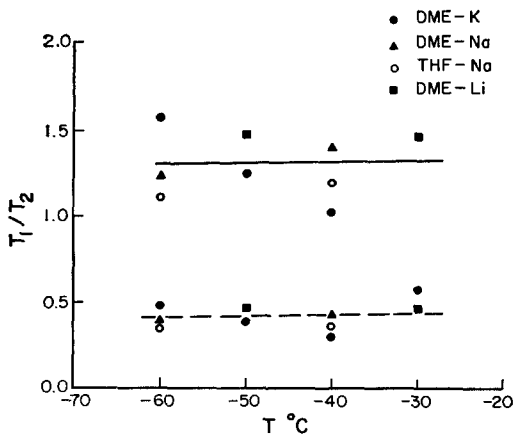

FIG. 7. T_1/T_2 variation for triphenylene negative ion as a function of temperature, solvent, and counterion.

lated spin densities (1.45) agrees quite well with the ratio of the splittings (1.50). Using $Q_{CH}{}^{H}=-27$ G [10,27] in the McConnell equation,[28] the experimental spin densities at the 1 and 2 positions are 0.060 and 0.040, respectively.

The central portion of the TP ESR spectrum also has the problem of overlap, so in order to obtain true relaxation times a procedure similar to the one employed for coronene was adopted. For obtaining peak-to-peak derivative widths from computer simulations, true imput widths from 250 to 700 mG were employed and computations were made at 20-mG intervals. In this case also, the widths may be related by a linear equation in the region of interest,

$$\delta_{true}=(2.332\pm0.058)\delta_{measured}-(0.270\pm0.018)\text{ G}. \quad (3.5)$$

Corrections for the experimentally measured peak-to-peak widths were made using Eq. (3.5). The results on the variation of T_1/T_2 using the corrected widths (upper curve) and also the uncorrected widths (lower curve) are shown in Fig. 7. The least-squares fit of our data to a straight line for T_1/T_2 for TP as a function of temperature is given by

$$T_1/T_2=(1.35\pm0.32)+(0.00073\pm0.0065)t\ ^\circ\text{C}. \quad (3.6a)$$

Here the temperature dependent term is clearly insignificant. A least-squares fit of T_2 (plotted in Fig. 5) vs t yields

$$T_2=[(1.79\pm0.04)-(0.0013\pm0.0011)t\ ^\circ\text{C}]\times10^{-7}. \quad (3.6b)$$

d. Cyclo-octatetraene. The cyclo-octatetraene anion radical (COT) has been extensively investigated by several authors in the recent past.[6,29] In the present experiments, we have generated the radical anion using Li reduction in DME and THF, Na reduction in DME, and also electrolytic reduction in DME. Dilute solutions of the radical have been employed for saturation measurements. However, when COT anion is produced by alkali metal reduction, the concentration of the radical varies with temperature.[6,29b,29c] The electrolytically reduced samples do not show any temperature-dependent concentration variations, and we used a sample $\approx10^{-4}M$ in COT for saturation studies. Relaxation times for COT depend strongly on the temperature at which they are determined, and also on the method by which the radical is generated. However, for the electrolytic sample the variation in the relaxation times is negligible between -40°C to room temperature. The values at -60 and -70°C are slightly higher, but at these temperatures much of the supporting electrolyte starts precipitating out of solution and the results obtained at these temperatures are not strictly to be compared with the numbers obtained above -40°C. Figure 8 shows the variation of T_1/T_2 as a function of temperature for the different samples of COT, and Fig. 9 shows the variation in linewidth as a function of temperature for COT samples produced by different methods. Figure 9 also contains linewidth variations in three very dilute samples of COT: DME–electrolytic, DME–Li, and THF–Li. These samples were made by diluting a $10^{-4}M$ solution in the sidearm of the sample tube to such an extent that no decrease in width was observed on further dilution. The signal-to-noise ratio in the ESR spectra from these

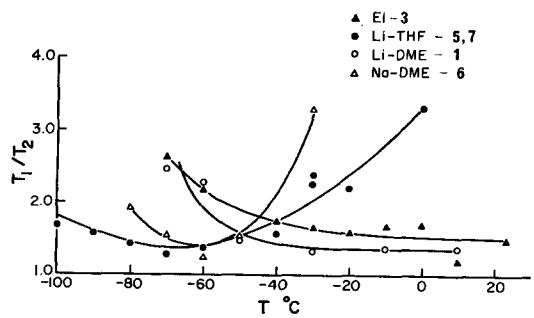

FIG. 8. T_1/T_2 variations for cyclooctatetraene anion. The numbering of samples refers to that of Fig. 9.

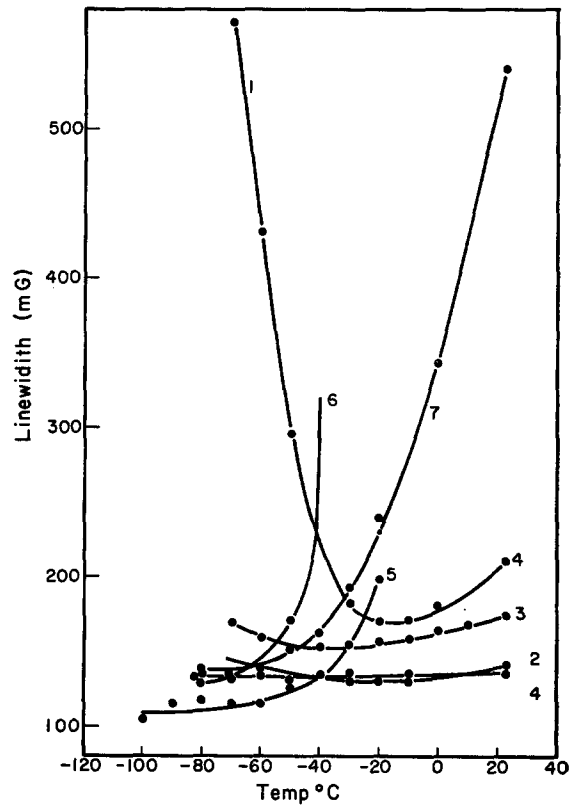

FIG. 9. Linewidth variations in cyclo-octatetraene negative ion as a function of temperature solvent and counterion. (1) COT–Li in DME, conc., see Curve 1, Fig. 10; (2) COT–Li in DME, dilute, see Curve 2, Fig. 10; (3) COT–electrolytic, 10^{-4} M in initial COT concentration; (4) COT–electrolytic, dilute, see text; (5) COT–Li in THF, dilute, see text; (6) COT–Na in DME, see Curve 6, Fig. 10; (7) COT–Li in THF, conc., see Curve 7, Fig. 10.

TABLE II. Representative relaxation times for systems investigated.[a]

Radical	T_1/T_2[b]	$T_1\times10^7$ sec	$T_2\times10^7$ sec[h]	$T_2\times10^7$ sec[i]
Benzene[b]	1.29±0.09	1.53	1.19±0.01	2.12
Coronene[c]	1.29±0.35	0.97	0.75±0.02	0.77
Triphenylene[c]	1.11±0.18	1.93	1.74±0.05	1.88
COT (electrolytic)[d]	1.58±0.09	6.70	4.20±0.10	5.06
COT (THF–Li)	1.36±0.07	6.64	4.89±0.06	6.58
p-Xylene[b,e,f]	1.78±0.50	19.4	10.9±0.1	13.28
Perinaphthenyl[g]	1.79±0.39	30.5	17.1±0.5	41.1
Naphthalene (DME–Na)	2.52±0.44	35.8	14.0±0.3	32.9
Tetracene (DME–K)	5.04±0.39	56.7	11.2±0.2	29.9
TCNE	3.13±0.21	81.0	25.9±0.5	82.2

[a] Results for measurements at −60°C if not specified otherwise.
[b] In 2:1 THF:DME with Na–K alloy.
[c] Results independent of solvent or counterion.
[d] Measured at −20°C. Results independent of temperature between (−40)–(23)°C (see text).
[e] Results at −70°C (see text).
[f] A minimum width corresponding to $T_2=13.2\times10^{-7}$ sec has been observed for toluene also (G. K. Fraenkel, private communications).
[g] In toluene at −20°C.
[h] Errors are sample deviations.
[i] Computed from the minimum measured widths.

dilute solutions was poor, and no saturation measurements were made on these samples. Figure 10 shows the concentration variation of COT as a function of temperature when different solvents and counterions are used for producing the radical (DME–Na, DME–Li, and THF–Li). It is clear from Fig. 9 that concentration-dependent contributions are affecting the widths of the more concentrated samples. Thus, they must also be affecting the T_1/T_2 ratios somewhat for these samples as shown in Fig. 8. The low concentration widths for COT:DME–electrolytic and DME–Li, are rather temperature independent, while those for COT:THF–Li are still quite temperature dependent above −50°C.

The concentration of each sample was determined at −30°C by comparison with a $10^{-4}M$ solution of K–TCNE in DME. The absolute concentration of

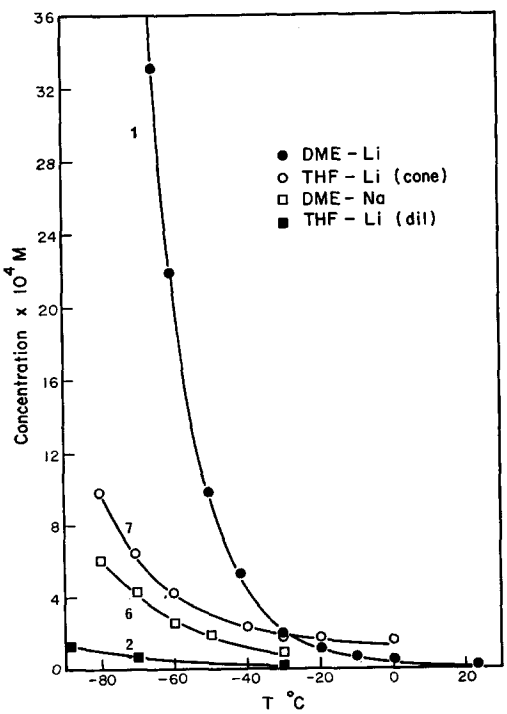

FIG. 10. Concentration variations in cyclo-octatetraene mononegative ion as a function of temperature in COT–alkali metal systems. The numbers corresponding to the different curves refer to the same numbers defined under Fig. 9.

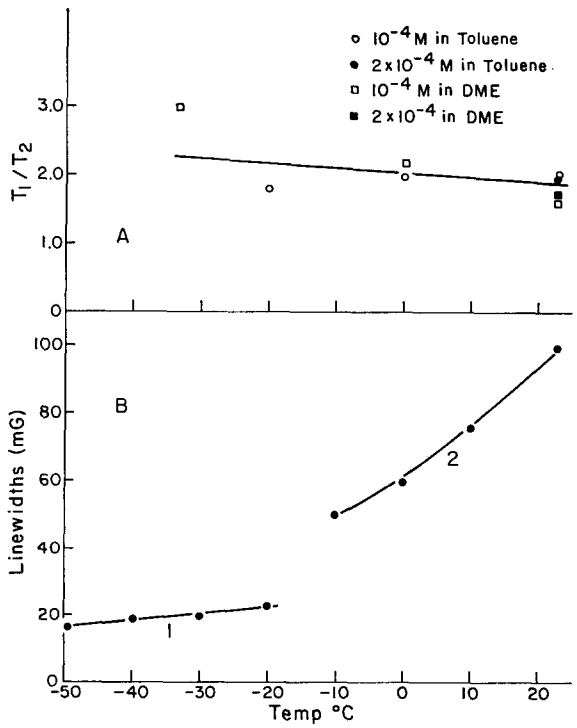

FIG. 11. T_1/T_2 variations (A) and linewidth variations (B) in perinaphthenyl. (1) Below −20°C the central component is resolved and second-order splittings were observed. (2) Above −10°C the lines are broader and no second-order splittings are observed. Solid points correspond to 10^{-4} *M* solutions at 23°C and the others refer to 2×10^{-4} *M* solutions at 23°C; see text.

TCNE was determined using uv measurements.[15] After obtaining the concentration of a given sample at −30°C, for all the other temperatures relative concentrations with respect to the −30°C concentration was obtained using the product of the first derivative amplitude and the square of the peak-to-peak width of the central line in the ESR spectrum as a measure of the concentration. Changes in audio gain settings and amplitude modulation were assumed to be linear,[30] and necessary corrections were applied for taking these changes into account.

2. Radical Anions with Nondegenerate Ground States

a. p-Xylene. The concentration of *p*-xylene negative ion in a mixture of THF and DME when produced by the reduction of *p*-xylene using Na–K alloy increases as the temperature is lowered in a manner similar to the benzene anion. However, unlike benzene anion, below −60°C, the *p*-xylene lines sharpen considerably, and at −70°C a width of 50 mG for a hyperfine component is observed. Using the central group of lines in the quintet spectrum of *p*-xylene the relaxation times were measured and the results are given in Table II, along with results for other radicals. In determining the T_1/T_2 ratio for *p*-xylene the peak-to-peak derivative widths of the envelope of the partially resolved central group of the quintet spectrum of *p*-xylene were employed. T_2 was obtained from the width of a *single* component of the central group, and it was assumed that the ratio of T_1/T_2 for the component is essentially the same as that for the envelope. The value of T_1 reported in Table II is obtained from this ratio.

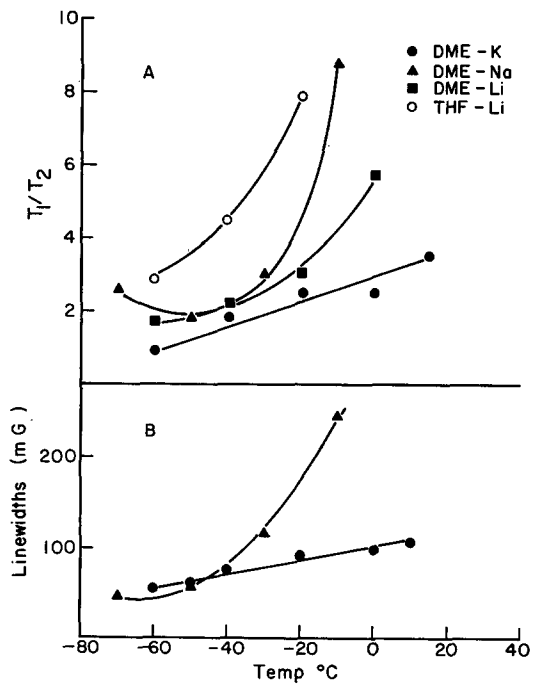

FIG. 12. T_1/T_2 variations (A) and linewidth variations (B) in naphthalene–alkali metal systems, $\approx 10^{-4}$ *M* in naphthalene negative ion. (see text).

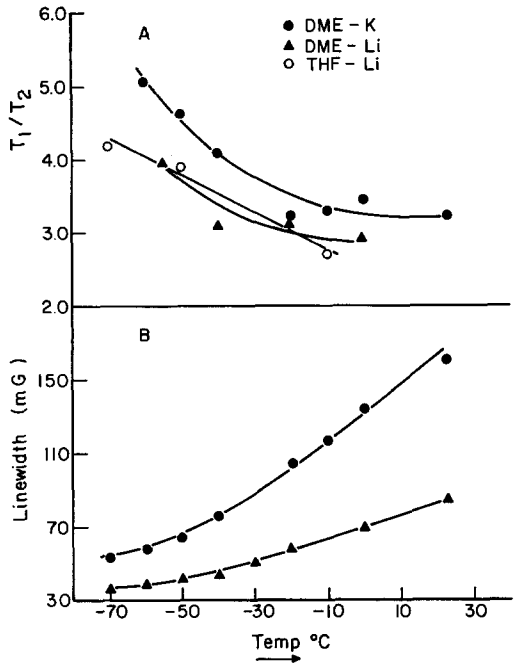

FIG. 13. T_1/T_2 variations (A) and linewidth variations (B) in tetracene–alkali metal systems, $\approx 10^{-4}$ *M* in tetracene negative ion (see text).

b. Perinaphthenyl. Relaxation times for perinaphthenyl in DME and toluene were measured between −33°C and room temperature. The results are shown in Fig. 11. When a solution of perinaphthenyl in DME or toluene is cooled, the concentration of the radical decreases at low temperatures as a result of dimerization.[31] As a consequence, when dilute solutions were employed for saturation studies at −40°C or below, the concentration is so low that the signal-to-noise ratio is poor. Thus, it is difficult to perform good saturation studies below −40°C in dilute solutions. However, we have determined the linewidth variation for a solution down to −50°C, and the result is shown in Fig. 5 (see Curve 1). The lines are extremely narrow at low temperatures, and one can observe second-order splittings, in both DME and toluene solutions, below −20°C. The curve is shown in an expanded scale on Fig. 11(b) (Curve 1). The results with a more concentrated sample ($2\times10^{-4}M$ at room temperature) between −10°C and room temperature are also shown in Fig. 11(b) (Curve 2).

c. Naphthalene and tetracene. The negative ions of naphthalene and tetracene have been examined in great detail under a variety of conditions by previous workers,[32–39] and considerable amount of information is available on the nature of their ESR spectra, ion-pairing effects, and splitting constants.

The results of saturation studies on solutions of naphthalene negative ion ($0.8–1\times10^{-4}M$) for four dif-

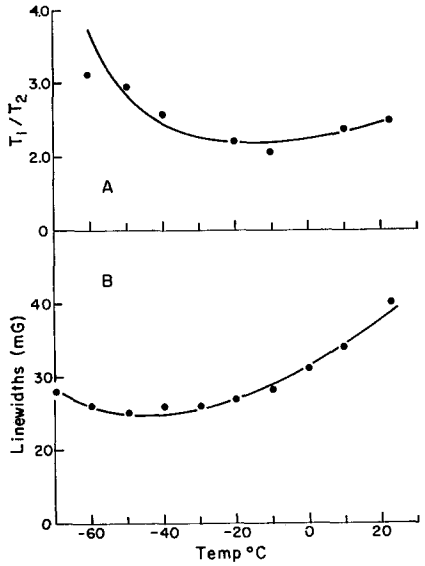

FIG. 14. T_1/T_2 variations (A) and linewidth variations (B) in $10^{-4}M$ K^+ TCNE in DME.

ferent systems, K–DME, Na–DME, Li–DME, and Li–THF, are given in Fig. 12(a). Figure 12(b) shows the linewidth variations of two of these systems, K–DME and Na–DME. As can be seen from Fig. 12(a), maximum variation in T_1/T_2 ratio is observed for naphthalene in DME when Na and K are used as counterions. As in these cases, the shapes of the linewidth curves for naphthalene–Li also closely follow the shapes of the T_1/T_2 curves. These are not included in Fig. 12(b) to avoid overcrowding at the low-temperature region. In the temperature range in which the saturation measurements have been done there was no overlap problem, and hence no corrections were necessary.

The results on tetracene negative-ion solutions (0.8–$1\times10^{-4}M$, K–DME, Li–DME, and Li–THF) are shown in Figs. 13(a) and 13(b). Figure 13(a) shows a plot of T_1/T_2 as a function of temperature for the three systems, while included in Fig. 13(b) are the typical linewidth variations in two of these systems, K–DME and Li–DME. The linewidth variation for Li–THF is essentially the same as that for Li–DME, and is not included in Fig. 13(b).

The tetracene anion spectrum at higher temperatures (-20)–(23)°C were simulated using experimental splittings and widths in order to check whether there exists any overlap problem at these temperatures at which the widths are larger, but no correction was found necessary.

d. K^+TCNE^-. Extensive saturation studies have been made on K^+TCNE^- in DME.[15] However, for comparison with our results on hydrocarbon radicals we have determined the relaxation times for a $10^{-4}M$ solution of K^+TCNE^- at different temperatures. T_1/T_2 for the $10^{-4}M$ sample as a function of temperature is shown in Fig. 14(a). Figure 14(b) contains a plot of the linewidth variation with temperature for this sample (see also Curve 2 in Fig. 5).

Typical values for relaxation times for the radicals discussed in this section are found in Table II.

C. ENDOR and ELDOR Results

Only the benzene anion in THF:DME was studied by these techniques. The ENDOR was run for a variety of concentrations and temperatures under conditions which give good signals in other radical systems (e.g., *p*-benzosemiquinone in DME),[18] but no discernible signal was ever obtained. ELDOR experiments were performed according to the method described by Eastman, Bruno, and Freed[17b] for two different concentrations. For a solution initially $1.0M$ in benzene with THF–DME solvent at -50°, a value of the reduction factor (obtained from an extrapolation to infinite pump power) of $R_\infty^{-1}=4.1\pm0.8$ (or a 24% reduction) was found. Here the $\tilde{M}=+1$ line was observed and the $\tilde{M}=-1$ line was pumped. When an initial concentration of $0.1M$, benzene was used at -60°C, the result was $R_\infty^{-1}=27\pm14$ (or a 3.7% reduction). Here the $\tilde{M}=0$ line was pumped, and the $\tilde{M}=+2$ line was observed. These results strongly indicated that the reductions are the result of a concentration dependent mechanism, viz., electron exchange with unreduced benzene. We can analyze R_∞ in terms of the relation appropriate for any exchange processes[17b]:

$$R_\infty^{-1}=(b''^{-1}/D_p)+1, \tag{3.7}$$

where $b''=\omega_{ex}/NW_e$, N is the total number of spin eigenstates (128 for benzene), ω_{ex} is the exchange frequency, W_e is the lattice-induced electron spin-flip rate, and D_p is the degeneracy of the pumped line. Utilizing $W_e=1/2T_1(0)=1.9\times10^{-7}$ sec^{-1}, one obtains $\omega_{ex}=7.2\times10^6$ sec^{-1} in the concentrated and 6.4×10^5 sec^{-1} in the dilute solution. Thus, the dilute solution, with a measured linewidth of 0.56 G, has only 0.32 G contributed by the exchange. (The concentrated solution of width 0.95 G is found to have an exchange contribution of 0.36 G.)

IV. DISCUSSION AND CONCLUSIONS

The results described in the previous section show some definite and interesting trends in the spin-relaxation characteristics of the hydrocarbon anions. Among those with degenerate ground states, TP and coronene exhibit a striking independence in the value of the T_1/T_2 ratio as a function of temperature, solvent, or counterion. This is also evidenced by benzene below -60°C and by COT between -40° and $+23$°C, when generated electrolytically. (Below -40°C the precipitation of electrolyte probably affects the results.) The values for T_1/T_2 are of the order of unity in these cases: 1.1 for benzene, 1.62 for coronene, 1.35 for tri-

phenylene, and 1.57 for COT (electrolytic). The deviations of these values from unity are not deemed very significant when one considers our estimate of 20%-30% absolute error for unoverlapped lines and an expected further error in large overlap corrections.

What is perhaps an even more significant result is that in the cases just noted the individual values of T_1 and T_2 are themselves *independent* of temperature, as well as solvent and counterion. This is most explicitly demonstrated in the coronene and TP systems. Furthermore, these temperature-independent T_1's and T_2's are shorter by an order of magnitude than those for the nondegenerate ground-state molecules (cf. Table II). The values of T_1 and T_2 for COT are nearly intermediate between the two groups. We note, however, in Fig. 9 that the different COT systems tend toward a common value of T_2^{-1} at lower temperatures, and this value is comparable to that for the electrolytic sample.[39,40]

The results for *p*-xylene (as well as for toluene) show that the minimum T_2^{-1} is reduced by more than a factor of 6 as compared to benzene. This is still of the order of a factor of 2 greater than for naphthalene and tetracene and suggests that the splitting of the orbital degeneracy of benzene by the methyl groups probably does not entirely remove the anomalous relaxation effects. (The T_1 and T_2 are comparable for *p*-xylene within experimental error.)

Before discussing the implications of the above observations, we note that in the cases of benzene above -60°C and COT generated by alkali metal reduction, there are strong temperature variations, but they are primarily in T_2. One finds T_2^{-1} (or the linewidth) increases rapidly with temperature (cf. Fig. 5), as does T_1/T_2.[41] A comparison with the results for nondegenerate ground-state hydrocarbons (Figs. 5, 11–14) shows that there is similar behavior for the naphthalene—especially (Na–DME) system, but the tetracene systems show much less pronounced effects. Rather less sensitive to temperature changes are the T_2's for the neutral radical perinaphthenyl and for K^+TCNE^-.[42]

The rather slim possibility that the width increase with increasing temperature of the lower concentration benzene samples might be due to some unusual chemical exchange process was raised in Part I. Our ELDOR results reported in Sec. III, however, show definitely that exchange-dependent contributions to the width are negligible in the lower concentration (0.1*M* or less) benzene samples, so they cannot be the source of the temperature-dependent increasing widths. We note also that our negative ENDOR results should also imply the unimportance of nuclear spin-dependent relaxation processes [e.g., contributions from anisotropic but especially isotropic dipolar interactions] in the T_1's and T_2's for the benzene anion.[18,43]

Malinoski and Bruning[44] (MB) have recently suggested that the increase in T_2^{-1} with temperature above -60°C for benzene anion may be due to ion-pairing effects, viz., residual broadening from unresolved alkali metal hyperfine structure. Ion pairing between hydrocarbon anions and alkali metals is a well-characterized phenomenon.[32,24–39,45–49] The basic mechanism could be a rapid cation exchange: $R^-M^+ + M^+ \rightleftarrows M^+ + R^-M^+$. MB called attention to the T/η dependence of T_2^{-1} as possible evidence of this, if the exchange were diffusion controlled; while in Part I their suggestion was criticized, our present results tend to support the basic mechanism, but as analyzed somewhat differently from MB. Thus our earlier criticism included the following: (1) There is the apparent solvent independence of the widths for benzene; (2) rather large values of alkali metal splitting "*a*" for ^{39}K (but not for ^{23}Na) would be required, or else inhomogeneous broadening of the lines should be occurring—but this was not detected; and (3) if the mean ion-pair lifetime τ_2 were diffusion controlled, $\tau_e \propto \eta/T$, so that by the equation for the linewidth contribution in the exchange-narrowed region (for $I=\frac{3}{2}$),[50]

$$T_2^{-1}(I.P.) = (5/4)\,pa^2[\tau_e + \tau_e/(1+\omega_0^2\tau_e^2)] \quad (4.1)$$

(where p is the probability of the anion existing as an ion-pair), the linewidth should *decrease*[51] with increasing T when $\omega_0^2\tau_e^2 \gg 1$, in contradiction to both the experimental observation and the suggestions of MB. The inequality $\omega_0^2\tau_e^2 \gg 1$ would be required by the fact that this mechanism leads to a T_1 contribution,[50]

$$T_1^{-1}(I.P.) = \tfrac{5}{2}pa^2\tau_e/(1+\omega_0^2\tau_e^2), \quad (4.2)$$

and from the experimental results the temperature-dependent mechanism must fulfill $T_1(I.P.) \gg T_2(I.P.)$. Actually the T/η dependence in the benzene case may just be fortuitous. Thus, an equally good linear fit to the linewidth data was achieved[1] as a function of T. Further, our careful linewidth study (Fig. 2) of benzene in several related solvents shows a small, but nontrivial, solvent effect. Also, as may be seen in Figs. 9 and 12, the similar strong temperature-dependent contributions to T_2^{-1} for COT, naphthalene, etc., do not vary in accordance with a T/η dependence.[52] Our current observations of temperature-dependent line shape changes for the benzene anion at the higher temperatures (cf. Fig. 3) are consistent with an increasingly inhomogeneously broadened width as the temperature is increased. This suggests that $pa^2\tau_e^2$ is increasing with temperature and is becoming greater than unity[50,53] in accordance with the ion-pairing model.

Our results do strongly suggest that ion-pairing effects are making a significant contribution to T_2^{-1} without making an important contribution to T_1^{-1}. The variations in our results with radical, solvent, and counterion are reasonably well correlated with the already demonstrated trends[34–36] that association between a hydrocarbon negative ion and an alkali metal ion increases with (1) decreasing size of the hydrocarbon, (2) increasing radius of the cation (although

TABLE III. Results of least-squares fits of minimum widths of hydrocarbon radicals with degenerate ground states as a function of g-value variations.

Independent variable[a]	Slope	% Error	Intercept	% Error
$f(\Delta g)^{b,c}=(g_{exptl}-g_{theoret})$	0.0188±0.0002	1.2	0.212±0.003	1.7
$f(\Delta g)^{b,d}=(g_{exptl}-g_{theoret})^2$	0.0005±0.0001	21.0	0.215±0.058	27.0
$f(\Delta g)^{c,e}=(g_{exptl}-g_e)$	0.015±0.003	18.0	−0.38±0.13	36.0
$f(\Delta g)^{d,e}=(g_{exptl}-g_e)^2$	0.0155±0.0014	9.0	−0.046±0.004	9.0

[a] Least-squares fit to the equation: $\delta=mf(\Delta g)+b$, where δ is the linewidth in gauss, $f(\Delta g)$ is the g-value variation, m is the slope, and b is the intercept.

[b] g_{exptl} is the experimental g value of the hydrocarbons, and $g_{theoret}$ is the g value as predicted using Stone's theory (see text).

[c] $f(\Delta g)$ in units of 10^{-5}.

[d] $f(\Delta g)$ in units of 10^{-8}.

[e] g_e is the g value of the free electron (see text).

the perturbation of the hydrocarbon ion will be greater for a cation with a smaller radius), (3) increasing temperature, and (4) decreasing solvent coordination of the metal ion (i.e., DME solvates metal ions better than THF).

The over-all temperature dependence of the ion-pair broadening mechanism as given by Eq. (4.1) would be rationalized in terms of either an equilibrium constant for ion-pairing, $M^+R^- \rightleftarrows M^+ + R^-$, which favors ion-pairing at the higher temperatures, thus increasing p, and/or an increasing "a" with temperature,[37–39] possibly due to an increase in tight vs loose ion pairing. Large increases in these parameters could more than offset the expected decrease in τ_e with T.[53] While a more detailed analysis of our solvent- and counterion-dependent results could be of interest with regard to the details of ion-pairing mechanisms, we have not pursued the matter further.

Our main observation is that when temperature-dependent ion-pairing width effects are removed, and when concentrations are low enough to preclude exchange effects, then each ground-state degenerate free radical in liquid solution is characterized by a T_2^{-1} (with a comparable T_1^{-1}) which is virtually independent of all other external variables, e.g., solvent, temperature, and counterion. These linewidths are strictly characteristic of the particular radical. We can therefore attempt to correlate these temperature-independent widths with other physical parameters. Since the only proposed mechanisms which have not by now been categorically ruled out, all involve a spin–orbit interaction [e.g., McConnell's spin–orbit pulse (SOP)[2], Kivelson's Orback-type (KO)[3], and the spin–orbit tunneling (SOT) mechanism[4,5]], a correlation with the g shifts of these radicals would be in order. However, since the mechanism is anomalous in that it is not making a comparable contribution for the nondegenerate hydrocarbons, this may not be the most meaningful correlation. It has been pointed out that the various spin–orbit processes would be associated with anomalous deviations in g shift (Δg) which could be small.[4] This prediction is in keeping with the results of Segal, Kaplan, and Fraenkel on careful measurements of g values.[16] They found that the Δg values for a set of 11 nondegenerate ground-state hydrocarbon radicals could be fitted to a semiempirical relation proposed by Stone[54]:

$$\Delta g=\bar{g}-g_0=[31.9\pm0.4-(16.6\pm1.0)\lambda]\times10^{-5}, \quad (4.3)$$

where g and g_0 are the experimental and free electron g values, and in the Hückel theory for aromatic hydrocarbons the energy of the molecular orbital occupied by the unpaired electron is written as

$$E=\alpha+\lambda\beta. \quad (4.4)$$

Here α and β are the Coulomb and exchange integrals

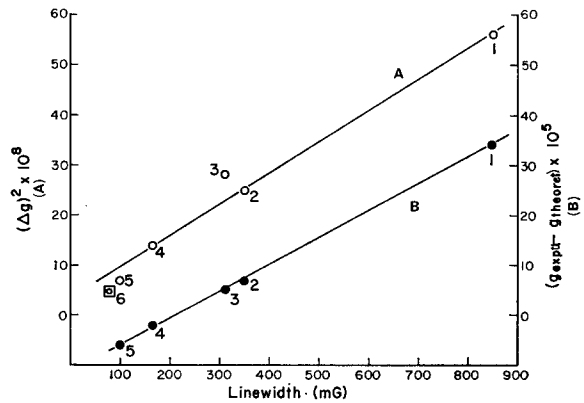

FIG. 15. Minimum linewidths for hydrocarbon negative ions with degenerate ground states as a function of g-value variations. Curve A shows the correlation of linewidths with [g(experimental) − g(free electron)]^2, and Curve B shows the correlation of the widths with [g(experimental) − g(theoretical)] where g(theoretical) is the value calculated using Stone's theory; see text. The points shown in the figure are (1) coronene (Ref. 16); (2) triphenylene (present work); (3) benzene anion (Ref. 16); (4) tropenyl [M. K. Carter and G. Vincow, J. Chem. Phys. **47**, 292 (1967)]; (5) cyclo-octatetraene (Ref. 16); (6) cyclopentadienyl [P. J. Krucic and J. K. Kochi, J. Am. Chem. Soc. **90**, 7155 (1968)]; the g value of this radical in solution has not been determined and hence the point (calculated using Stone's theory) is shown as a square in Curve A and not included in Curve B. Except for (4) and (6), in all other cases the minimum widths reported are from the present experiments. For (4) and (6) the values reported in the corresponding references cited above have been employed.

for carbon, respectively. They found, however, that coronene, benzene, and COT exhibit significant (although fairly small) discrepancies from the prediction of Eq. (4.3). We have considered the correlation of the widths with ϵ where

$$\epsilon = \Delta g_E - \Delta g_s, \tag{4.5}$$

and Δg_E and Δg_s are the experimental Δg and that predicted by the Stonetype relation Eq. (4.3), respectively. The deviations ϵ are both positive (coronene, TP, and benzene) and negative (COT and tropenyl). An analysis of all the proposed spin–orbit mechanisms shows that they arise in the same order in (generalized) perturbation theory as the associated g shifts, the latter being the dynamic frequency shifts associated with the relaxation terms.[5] Thus, a linear relation between Δg_E or ϵ and T_2^{-1} might be expected. The results of such least-squares fits for five ground-state degenerate free radicals are summarized in Table III. Only a fair fit is achieved with Δg_E, but a surprisingly good fit is obtained with ϵ (% deviation of about unity). When fits of Δg_E^2 and ϵ^2 with T_2^{-1} were attempted, the agreement with Δg_E^2 is improved (9% deviations), but that for ϵ^2 is no longer very good (25% deviation). The two best fits are shown in Fig. 15. (Note that normal g-tensor and spin–rotational type relaxation mechanisms are essentially quadratic in Δg, or more precisely, they vary as the sums of squares of deviations of the principal components of g from the $\bar{g}$ and g_0, respectively.[51,55] This is because they appear in higher order in generalized perturbation theory.)[5,56] We note that while g-tensor type effects have been ruled out by field-frequency-dependent studies, as the dominant contribution to the anomalous widths,[1,57] anomalous spin–rotational effects arising from unusual spin–orbit terms have not been ruled out.

The correlations of Table III and Fig. 15 are believed to be the first positive evidence supporting the hypothesis that the anomalous linewidths are indeed due to some anomalous spin–orbit-type process(es). The excellent correlation between ϵ and T_2^{-1} encourages one to take more seriously the proposed spin–orbit mechanisms which depend upon orbital (near) degeneracy.[2–5] Furthermore, the reasonable correlation of T_2^{-1} with Δg_E (which is not in serious disagreement with Δgs) suggests that the anomalous spin–orbit terms may be generated by spin–orbit interaction between π and σ^* (or σ) orbitals involved in the ground and excited states. One such proposal by Kivelson involves cross terms between an orbit–lattice and spin–orbit interaction.[3] We have considered[5] the possible effects of vibronic-spin–orbit terms, which are deemed important in the phosphorescence decay of triplet benzene to its ground state.[58] In the present case, this would involve vibronic mixing of ground and highly excited states in place of orbit–lattice mixing.[59]

We next consider the remarkable solvent, counterion, and temperature independence of these widths. This would suggest that the relaxation mechanism is predominantly intramolecular. The existence of intramolecular vibronic relaxation for medium-sized molecules, which is temperature independent, has been the subject of considerable investigation recently.[60] Since the vibronic levels would be expected to have temperature- and solvent-independent natural widths ω^*, the inverse widths ω^{*-1} can then serve as an appropriate correlation time for spin-relaxation processes involving a vibronic-spin–orbit interaction.[5] On the other hand, an orbit–lattice interaction would not be expected to be consistent with our results. Although rotational averaging is very important in liquid spin relaxation,[4] the fact that one expects $\omega^* \gg \tau_R^{-1}$, where τ_R is a rotational correlation time, means that the over-all correlation time would still be dominated by ω^{*-1}, even while spin–orbit effects are being rotationally averaged.

We note that the original proposals of McConnell,[2] Kivelson,[3] and Freed and Kooser[4] were all based on important solvent (and counterion) dependences. Thus, these proposals as originally given do not appear appropriate considering our observation that solvent and counterion are not important. Nevertheless, the basic schemes, especially for the KO and SOT mechanisms, can still be applied to the intramolecular vibrational degrees of freedom instead of intermolecular solvent and counterion modes of motion.[5] A vibronic-spin–orbit interaction would necessarily require such a modification. A comprehensive analysis of these different spin–orbit mechanisms will be given elsewhere.[5]

ACKNOWLEDGMENTS

We wish to thank Mr. Henry D. Connor for performing the ENDOR measurements and Mr. Gerald V. Bruno for performing the ELODR measurements.

* Supported in part by the Advanced Research Projects Agency and by PHS Research Grant No. GM 14123 from the National Institutes of Health.

[1] R. G. Kooser, V. W. Volland, and J. H. Freed, J. Chem. Phys. **50,** 5243 (1969).
[2] H. M. McConnell, J. Chem. Phys. **34,** 13 (1961).
[3] D. Kivelson, J. Chem. Phys. **45,** 751 (1966).
[4] J. H. Freed and R. G. Kooser, J. Chem. Phys. **49,** 4715 (1968).
[5] J. H. Freed (unpublished).
[6] R. G. Lawler, M. R. Das, L. C. Siew, and G. K. Fraenkel (unpublished).
[7] (a) R. G. Lawler, J. R. Bolton, and G. K. Fraenkel, J. Am. Chem. Soc. **86,** 520 (1964); (b) R. G. Lawler, J. R. Bolton, G. K. Fraenkel, and T. H. Brown, J. Chem. Phys. **49,** 1126 (1968).
[8] V. Boekelheide and C. E. Larrabee, J. Am. Chem. Soc. **72,** 1245 (1950).
[9] P. H. Reiger, I. Bernal, W. H. Reinmuth, and G. K. Fraenkel, J. Am. Chem. Soc. **85,** 683 (1963).
[10] J. R. Bolton and G. K. Fraenkel, J. Chem. Phys. **40,** 3307 (1964).
[11] J. R. Bolton, Mol. Phys. **6,** 219 (1963).
[12] D. E. Paul, D. Lipkin, and S. I. Weissman, J. Am. Chem. Soc. **78,** 116 (1956).

[13] P. Balk, G. J. Hoijtink, and J. W. H. Schreurs, Rec. Trav. Chim. **76,** 813 (1957).
[14] R. L. Ward, J. Am. Chem. Soc. **83,** 1296 (1961).
[15] M. P. Eastman, R. G. Kooser, M. R. Das, and J. H. Freed, J. Chem. Phys. **51,** 2690 (1969).
[16] B. G. Segal, M. Kaplan, and G. K. Fraenkel, J. Chem. Phys. **43,** 4149 (1965).
[17] (a) J. S. Hyde, J. C. W. Chien, and J. H. Freed, J. Chem. Phys. **48,** 4211 (1968); (b) M. P. Eastman, G. V. Bruno, and J. H. Freed, *ibid.* **52,** 329 (1970).
[18] D. S. Leniart, H. D. Connor, M. R. Das, and J. H. Freed (unpublished).
[19] J. W. H. Schreurs, G. E. Blomgren, and G. K. Franekel, J. Chem. Phys. **32,** 1861 (1960).
[20] (a) E. L. Ginzton, *Microwave Measurements* (McGraw-Hill, New York, 1957); (b) J. H. Freed, D. S. Leniart, and J. S. Hyde, J. Chem. Phys. **47,** 2762 (1967).
[21] Note that tables of the original data utilized in the figures may be found in S. B. Wagner, Master's thesis, Cornell University, Ithaca, N.Y., 1969.
[22] M. G. Townsend and S. I. Weissman, J. Chem. Phys. **32,** 509 (1960).
[22a] *Note added in proof:* Dr. van Broekhoven has kindly called attention to the work of H. van Willigen, J. A. M. van Broekhoven, and E. de Boer, Mol. Phys. **12,** 533 (1967), on the TP anion. Our results are consistent with what they call the type I or free anion.
[23] A. D. McLachlan, Mol. Phys. **3,** 233 (1960).
[24] The McLachlan calculations failed to produce meaningful results because the wavefunctions from the Hückel scheme used in the calculations predict equivalent spin density at each π-electron position in the molecule due to the symmetry of triphenylene. When the average is taken at each of the carbon centers of the two McLachlan calculations with the odd electron in each of the degenerate orbitals (symmetric and antisymmetric) the spin density contributions in the correction term factor out because of their equivalence in the Hückel approximation. What is left is the sum of the polarizabilities due to the carbon center in question, and this sum is equal to zero.
[25] (a) R. Pariser and R. G. Parr, J. Chem. Phys. **21,** 466, 767 (1953); (b) J. A. Pople, Trans. Faraday Soc. **49,** 1375 (1953); (c) C. A. Brickstock and J. A. Pople, Trans. Faraday Soc. **50,** 901 (1954).
[26] In the successive iteration procedure employed, the equations of Pople are used [Ref. 25(b), 25(c)] in which the electron–electron repulsion terms are included. A value of 2.39 eV was used for the Coulombic integrals [Ref. 25(a)], and the repulsion integrals were calculated using the methods of Pariser and Parr [Ref. 25(a)]. The iterations were carried out until agreement was reached in the fourth decimal position of both the unpaired spin densities and energies. The spin density of the odd electron was taken as an average over the degenerate orbitals after each iteration. After one iteration the spin densities were $\rho_1=0.058$ and $\rho_2=0.053$, and after 13 iterations the spin densities were $\rho_1=0.061$ and $\rho_2=0.042$. *Note added in proof:* This is consistent with the deuteration experiments of Ref. 22(a) that ρ_1 is the larger. Our numerical SCF results are somewhat different from theirs.
[27] (a) J. R. Bolton and G. K. Fraenkel, J. Chem. Phys. **40,** 3307 (1964); (b) M. R. Das and G. K. Fraenkel, *ibid.* **42,** 1350 (1965); (c) W. M. Gulick, Jr. and D. H. Gaske, J. Am. Chem. Soc. **88,** 4119 (1966); (d) B. S. Prabhananda, M. P. Khakhar, and M. R. Das, *ibid.* **90,** 5980 (1968); (e) P. D. Sullivan and J. R. Bolton, *ibid.* **90,** 5366 (1968); (f) C. A. Claxton and D. McWilliams, Trans. Faraday Soc. **64,** 2593 (1968).
[28] (a) H. M. McConnell, J. Chem. Phys. **24,** 632, 764 (1956); (b) H. M. McConnell and H. H. Dearman, *ibid.* **28,** 51 (1958); (c) H. M. McConnell and D. M. Chesnut, *ibid.* **28,** 107 (1958).
[29] (a) T. J. Katz, J. Am. Chem. Soc. **82,** 3784, 4785 (1960); (b) H. C. Strauss, T. J. Katz, and G. K. Fraenkel, *ibid.* **85,** 2360 (1963); (c) F. J. Smentowski and G. R. Stevenson, *ibid.* **89,** 5120 (1967).
[30] This was checked for each sample at −30°C for the range of audio gains and modulation amplitudes that were found necessary for the sample.
[31] F. Gerson, Helv. Chim. Acta **49,** 1463 (1966).
[32] N. M. Atherton and S. I. Weissman, J. Am. Chem. Soc. **83,** 1458 (1961).
[33] J. P. Colpa and J. R. Bolton, Mol. Phys. **6,** 273 (1963).
[34] K. H. J. Buschlow, J. Dielman, and G. J. Hoijtink, J. Chem. Phys. **42,** 1993 (1965).
[35] R. B. Slates and M. Szwarc, J. Phys. Chem. **69,** 4124 (1965).
[36] (a) P. Chang, R. V. Slates, and M. Szwarc, J. Phys. Chem. **70,** 3180 (1966); (b) K. Hofelmann, J. Jagur-Grodzinski, and M. Szwarc, J. Am. Chem. Soc. **91,** 4645 (1969).
[37] N. Hirota, J. Phys. Chem. **71,** 127 (1967).
[38] C. L. Dodson and A. H. Reddoch, J. Chem. Phys. **48,** 3226 (1968).
[39] P. Graceffa and T. R. Tuttle, Jr., J. Chem. Phys. **50,** 1908 (1969).
[40] Actually the minimum linewidth obtained for Li–COT in THF (at −100°C) of 100 mG is somewhat less than the value of 130 mG for the electrolytic and other samples. It could be possible that in this case (Li–COT in THF) the ion–radical interaction in sufficiently large to slightly remove the orbital degeneracy and reduce slightly the anomalous width.
[41] There is one exception to the general trends in T_2. In the concentrated solution of COT–Li in DME (see Fig. 9), the linewidth *increases* with decreasing temperature in the region of −15 to −70°C. (Above −15°C the normal trend of linewidth increase with temperature is observed.) The linewidth dependence below −15°C may be correlated with the very rapid increase in the radical concentration at low temperatures for this counterion–solvent system (see Fig. 10). The existence of the disprotortionation equilibrium $2R^{-}\rightleftharpoons R+R^{=}$ in COT-alkali metal systems is well known (Refs. 6, 29), and in Li–DME the reverse reaction becomes relatively more favorable at lower temperatures. It would not be unreasonable to conclude that the increased width at low temperatures is due to Heisenberg spin-exchange contributions which would normally vary as T/η if the spin concentration remained constant with temperature. The low-concentration COT–Li in DME sample (see Fig. 9) shows very little variation with temperature.
[42] In most cases for the nondegenerate ground-state radicals, T_1 increases at the lower temperatures as expected from normal g-tensor and spin–rotational T_1 mechanisms which vary as η/T. The largest variation was shown by TCNE in DME, and tetracene–Li in DME. The results of least-squares fits of T_1 to η/T for these two systems are: $(3.3\pm0.2)\times10^{-6}+(0.66\pm0.05)\eta/T\times10^{2}$ sec for TCNE, and $(1.2\pm0.4)\times10^{-6}+(0.75\pm0.08)\eta/T\times10^{2}$ sec for tetracene. In other cases either the T_1 variation was not very significant with temperature, or it did not show any systematic trends.
[43] J. H. Freed, J. Chem. Phys. **43,** 2312 (1965).
[44] G. L. Malinoski, Jr. and W. H. Bruning, J. Chem. Phys. **50,** 3637 (1969).
[45] (a) H. V. Carter, B. J. McClelland, and E. Warhurst, Trans. Faraday Soc. **56,** 455 (1960); (b) A. C. Aten, J. Dielman, and G. J. Hoijtink, Discussions Faraday Soc. **29,** 182 (1960); (c) C. J. McClelland, Trans. Faraday Soc. **57,** 1458 (1961); (d) E. deBoer and E. L. Mackor, J. Am. Chem. Soc. **86,** 1513 (1964).
[46] A. H. Reddoch, J. Chem. Phys. **41,** 44 (1964).
[47] T. E. Hogen Esch and J. Smid, J. Am. Chem. Soc. **87,** 669 (1965).
[48] A. H. Reddoch, J. Chem. Phys. **43,** 3411 (1965).
[49] N. Hirota and R. Kreilick, J. Am. Chem. Soc. **88,** 614 (1966).
[50] A. Abragam, *The Principles of Nuclear Magnetism* (Clarendon, Oxford, England, 1961), Chap. 8.
[51] One might also expect a further line broadening term from modulation of the proton hyperfine interaction, a_H, if the radical can exist for appreciable times in the non-ion-paired form. The expression is, however, dependent on the nuclear spin quantum numbers. Thus, for example, if all the nuclei remain completely equivalent, one has

$$T_2^{-1}(\mathrm{H}F)=(1-p)\,p^2(a_{\mathrm{H}}^{I\cdot P\cdot}-a_{\mathrm{H}}^{F})^2M^2\tau_F,$$

where $a_{\mathrm{H}}^{I\cdot P\cdot}$ and a_{H}^{F} are the hyperfine splittings in the ion-pair and free ion states, τ_F is the mean lifetime of the free ion, and M is the total nuclear-spin quantum number. This M dependence is contrary to experimental observation, so it would require $T_2^{-1}(\mathrm{H}F)$ to be unimportant. This would be the case, for example if $p\sim1$, i.e., the radical always exists as a simple ion pair. In this case τ_e^{-1} is simply the rate of counterion exchange.
[52] Note that if a straight-line least-square fit of log (residual width) vs $1/T$ is made, the following results are obtained for the activation energies: benzene: (Na–K alloy in THF–DME)

3.0±0.2 kcal/mole; COT: (Li–THF) 3.8±0.2 kcal/mole; tetracene: (Li–DME) 1.97±0.09 kcal/mole. The residual width is the difference between the observed width at a given temperature and the temperature-independent width of the same sample. A plot of $\log(\eta)$ vs $1/T$ on the other hand yields the activation energies DME: 1.97±0.14 kcal/mole, and THF: 1.83±0.14 kcal/mole. Notice that the values are, indeed, different for benzene and COT where ion pairing is expected to play an important role, but are closely similar for tetracene.

[53] J. H. Freed and G. K. Fraenkel, J. Chem. Phys. **39,** 326 (1963).

[54] A. J. Stone, Mol. Phys. **6,** 509 (1963); **7,** 311 (1964).

[55] P. W. Atkins and D. Kivelson, J. Chem. Phys. **44,** 169 (1966).

[56] J. H. Freed, J. Chem. Phys. **49,** 376 (1968).

[57] We have also performed ESR experiments at 35 GHz at −65 and at −20°C on several hydrocarbon anions, and it has been noticed that there is no significant linewidth differences for radicals with degenerate ground states at 35 GHz as compared to X-band results. The peak-to-peak derivative widths as 35 GHz for the central components of the ESR spectra of different radicals at −20°C are given below. Indicated in parentheses are the widths for the same samples at X band: Coronene, 0.93 G (0.92 G); benzene, 0.95 G (1.0 G); cyclooctatetrane, 0.44 G (0.23 G); tetracene–Li in THF, 0.23 G (0.08 G). At −65°C, the corresponding widths are as follows: coronene, 0.92 G (0.91 G); benzene, 0.63 G (0.47 G); cyclo-octatetraene, 0.33 G (0.15); tetracene, 0.23 G (0.056 G).

[58] A. C. Albrecht, J. Chem. Phys. **38,** 354 (1963).

[59] The McConnell mechanisms (Ref. 2) whereby a net L_z, characteristic of the sixfold symmetry, leads to an anomalous g_z is not consistent with the g-tensor measurements of Volland and Vincow [J. Phys. Chem. **73,** 1147 (1969)] on tropenyl. They find g_z for this radical is closely predicted by the Stone theory (Ref. 53). The above-noted mechanism, however, would lead to small anomalies in g_x and g_y.

[60] M. Bixon and J. Jortner, J. Chem. Phys. **50,** 4061 (1969), and references cited therein.

THE JOURNAL OF CHEMICAL PHYSICS VOLUME 52, NUMBER 10 15 MAY 1970

Study of Some Pr(III) Complexes: Interelectronic Repulsion, Spin–Orbit Interaction, and Bonding

S. P. TANDON AND P. C. MEHTA

Department of Physics, University of Jodhpur, Jodhpur, India

(Received 8 October 1969)

The values of Slater-Condon (F_2, F_4, F_6) and Racah (E^1, E^2, E^3) interelectronic repulsion and Landé (ζ_{4f}) parameters have been computed from the already observed visible and near-infrared absorption spectra of nineteen Pr(III) complexes. The decrease in F_2 values of the complexes as compared to the free ion is greatest among all the parameters and has been explained. The bonding parameter $b^{1/2}=[\frac{1}{2}(1-\beta)]^{1/2}$ has also been computed calculating a β value for each complex using the relation $\beta=F_k^c/F_k^f$, where F_k^c and F_k^f refer to the complex and the free ion, respectively. The relative variation of covalent bonding in the complexes has been discussed.

INTRODUCTION

Study of absorption spectra in visible and near-infrared regions yields[1] useful information regarding interelectronic repulsion, spin–orbit interaction, nephelauxetic effect, and bonding in complexes. However, such studies have been carried out in the case of very few rare earth complexes. It is only recently that the values of nephelauxetic ratio, β, in some Pr(III) complexes[2] and those of a bonding parameter, δ, using an empirical relation (Eq. 1) have been reported[3]

$$\delta=[(1-\beta)/\beta]100, \tag{1}$$

where the β values have been estimated using the approximate relation

$$\beta=\bar{\nu}_c/\bar{\nu}_f. \tag{2}$$

$\bar{\nu}_c$ and $\bar{\nu}_f$ are the energies of the internal f^2 transition bands of the complex and the free ion, respectively.

This article reports the values of Slater–Condon (F_k), Racah (E^k), Landé (ζ_{4f}), and bonding ($b^{1/2}$) parameters in the case of 19 Pr(III) complexes. The variation of these parameters in different complexes has been discussed.

CALCULATION OF PARAMETERS

The visible and near-infrared spectrum of Pr(III) arises[4] due to forbidden transitions within the ground $4f^2$ configuration. The energy level structure of $4f^2$ configuration, to a first approximation, may be considered to arise from electrostatic and magnetic interactions between the $4f$ electrons. The expansion of the electrostatic interaction term, E_e, in terms of Legendre polynomials enables one to express E_e [Eq. (3)] in terms of products of Slater radial integrals (also known as Slater–Condon parameters), F_k, and angular coefficients f^k

$$E_e=\sum_{k=0}^{6} f^k F_k=\sum_{k=0}^{6} f_k F^k. \tag{3}$$

F_k is given by

$$F_k=D_k^{-1}\int_0^\infty\int_0^\infty r_<^k/r_>^{k+1}R^2(r_1)\,R^2(r_2)\,dr_1dr_2, \tag{4}$$

where the subscripts 1 and 2 refer to electron 1 and 2, respectively, R is the $4f$ radial function, $r_<$ denotes the radius of the electron nearer the nucleus, $r_>$ denotes